Published for SISSA by Springer

Received: January 13, 2021
Revised: May 6, 2021
Accepted: June 11, 2021
Published: June 28, 2021

Pole-skipping and hydrodynamic analysis in Lifshitz, AdS_2 and Rindler geometries

Haiming Yuan and Xian-Hui Ge[1]

Department of Physics, College of Sciences, Shanghai University, 200444 Shanghai, China

E-mail: yuan_haiming@shu.edu.cn, gexh@shu.edu.cn

Abstract: The "pole-skipping" phenomenon reflects that the retarded Green's function is not unique at a pole-skipping point in momentum space (ω, k). We explore the universality of pole-skipping in different geometries. In holography, near horizon analysis of the bulk equation of motion is a more straightforward way to derive a pole-skipping point. We use this method in Lifshitz, AdS_2 and Rindler geometries. We also study the complex hydrodynamic analyses and find that the dispersion relations in terms of dimensionless variables $\frac{\omega}{2\pi T}$ and $\frac{|k|}{2\pi T}$ pass through pole-skipping points $(\frac{\omega_n}{2\pi T}, \frac{|k_n|}{2\pi T})$ at small ω and k in the Lifshitz background. We verify that the position of the pole-skipping points does not depend on the standard quantization or alternative quantization of the boundary theory in $\mathrm{AdS}_2 \times \mathbb{R}^{d-1}$ geometry. In the Rindler geometry, we cannot find the corresponding Green's function to calculate pole-skipping points because it is difficult to impose the boundary condition. However, we can still obtain "special points" near the horizon where bulk equations of motion have two incoming solutions. These "special points" correspond to the nonuniqueness of the Green's function in physical meaning from the perspective of holography.

Keywords: AdS-CFT Correspondence, Gauge-gravity correspondence, Holography and condensed matter physics (AdS/CMT), Holography and quark-gluon plasmas

ArXiv ePrint: 2012.15396

[1] Corresponding author.

https://doi.org/10.1007/JHEP06(2021)165

JHEP06(2021)165

Contents

1 Introduction

The holography and the AdS/CFT correspondence [1–4] provide a useful method to compute Green's function at strong coupling and quantum many-body systems [5–9]. The out-of-time-ordered correlation functions(OTOCs) have been used to investigate the holographic chaos [10–12]. A new aspect of quantum chaos has been found by using the AdS/CFT correspondence [13, 14]. We can study the holographic chaos by using the retarded Green's function. Green's function is not unique at a pole-skipping point in complex momentum space (ω, k) and this phenomenon is known as "pole-skipping" [15–17]. The retarded Green's function is given by

$$G^R(\omega, k)_{T^{00}T^{00}} = \frac{b(\omega, k)}{a(\omega, k)}. \tag{1.1}$$

The location of the special points make the coefficient $a(\omega_\star, k_\star) = b(\omega_\star, k_\star) = 0$. Then, the retarded Green's function becomes $G^R(\omega_\star, k_\star) = 0/0$. The Green's function depends on the slope $\delta k/\delta\omega$.

$$G^R = \frac{(\partial_\omega b)_\star + \frac{\delta k}{\delta \omega}(\partial_k b)_\star + \dots}{(\partial_\omega a)_\star + \frac{\delta k}{\delta \omega}(\partial_k a)_\star + \dots}. \tag{1.2}$$

So if we find the intersection of zeros and poles in the retarded Green's functions, we can obtain these special points. We can use the simpler method, the AdS/CFT duality, to solve special points from the bulk field equation [13, 14, 18, 19]. On the bulk side, there is no unique incoming mode at the horizon, similar to the "pole-skipping" phenomenon in holographic chaos.

These special points $(\omega_\star, k_\star)$ can be divided into two classes: one class involves positive imaginary frequencies, while the others are at negative imaginary frequencies. The upper-half ω-plane special point contains the information of quantum chaos. We can extract the Lyapunov exponent λ and the butterfly velocity v_B from it.

$$\begin{aligned} C(t, x) \simeq e^{\lambda(t - x/v_B)} &= e^{-i\omega_\star t + ik_\star x}, \\ \omega_\star := i\lambda, \qquad k_\star &:= i\frac{\lambda}{v_B}, \end{aligned} \tag{1.3}$$

where $C(t, x)$ is a OTOC. $\omega_\star$ and $k_\star$ denote the frequency and momentum at the "pole-skipping" point, respectively.

Although the special points locate at the lower-half ω-plane are not related to the information of quantum chaos, the retarded Green's functions are also not unique at these special points. The general pole-skipping points in the lower-half ω-plane are located at negative integer (imaginary) Matsubara frequencies $\mathfrak{w}_n = -in$ $(n = 1, 2 \dots)$, where $\mathfrak{w} = \frac{\omega}{2\pi T}$. These special points have been found in BTZ black hole [18], Schwarzschild-AdS spacetime [19], 2D CFT [20], a holographic system with the chiral anomaly [21], a holographic system at finite chemical potential [22], hyperbolic space [23], the large q limit of SYK chain [24] and anisotropic plasma [25]. The lower-half ω-plane pole-skipping points, which are at non-integer values of $i\mathfrak{w}$, have been found in 2D CFT [20] and the large q limit of SYK chain [24]. Although Green's functions at the non-integer values of $i\mathfrak{w}$, pole-skipping points can not be defined uniquely, since the incoming boundary condition is not unique. The Green's functions at the non-integer values of $i\mathfrak{w}$ pole-skipping points are not related to the incoming solution at the horizon [26]. So if we use the holographic near horizon analysis to calculate the lower half-plane pole-skipping points, we can just obtain the negative integer points.

We study the boundary retarded Green's function $G^R(\omega, k)$ of a conserved U(1) charge current operator J^μ with $\langle J^\mu \rangle = 0$. The conserved current J^μ on the boundary is dual to

JHEP06(2021)165

the bulk field A_μ in a black hole spacetime. In the linear response regime, we find the retarded Green's function $G^R_{zz}(\omega, k)$ [27]

$$G^R_{zz}(k_\mu) = \frac{\omega^2\sigma}{i\omega - D_c k^2}, \qquad k = k_z, \tag{1.4}$$

where σ is the DC conductivity, z is a spatial direction, and D_c is the diffusion constant of charge. The retarded Green's function has a hydrodynamic pole corresponding to the charge diffusion at very small momentum and frequency

$$\omega = -iD_c k^2. \tag{1.5}$$

For the momentum diffusion, the corresponding bulk canonical momenta $T^{\alpha\mu}$ yield the retarded correlator [27]

$$G^R_{\alpha z,\alpha z} = \frac{\omega^2\sigma}{i\omega - D_p k^2}, \tag{1.6}$$

where α is any spatial direction x, y and D_p is the diffusion of momentum. The hydrodynamic pole corresponding to the momentum diffusion at minimal momentum and frequency is given by

$$\omega = -iD_p k^2. \tag{1.7}$$

In [15], the upper half-plane pole-skipping point is $\omega_\star = i\lambda_L,\ k_\star = \sqrt{6}i\pi T$. The dispersion relation of hydrodynamic sound modes $\mathfrak{w} = v_B\mathfrak{k}$ passes through the upper half-plane pole-skipping point $(\mathfrak{w}_\star, \mathfrak{k}_\star)$ for the case of Schwarzschild-AdS$_5$ spacetime, where $\mathfrak{w} = \frac{\omega}{2\pi T}$ and $\mathfrak{k} = \frac{k}{2\pi T}$. In [18], it was shown that the hydrodynamic poles (1.5) and (1.7) pass through the pole-skipping points in the lower half-plane for the case of Schwarzschild-AdS spacetime. Ref. [25] shows that the dispersion relation which arises from the pole of the retarded Green's function associated with the transverse momentum density passes through the lower half-plane pole-skipping points in the background of anisotropic plasma. The pole-skipping points may be related to the hydrodynamic dispersion relation.

In this paper, we show that near horizon analysis not only applies to AdS spacetime but also to Lifshitz and Rindler geometry. The pole-skipping points are related to the hydrodynamic dispersion relations in Lifshitz geometry. In section 2, we calculate the lower half-plane pole-skipping points of tensor, Maxwell vector and Maxwell scalar mode in the background of the anisotropic system near Lifshitz points. The frequencies of these special points are located at negative integer (imaginary) Matsubara frequencies $\mathfrak{w}_n := \frac{\omega_n}{2\pi T} = -in$ $(n = 1, 2, 3\ldots)$. We study the complex hydrodynamic analyses. The analytic properties of the dispersion relations have been treated as Puiseux series in complex momentum [28]. We plot the hydrodynamic dispersion relations in terms of dimensionless variables $\frac{\omega}{2\pi T}$ and $\frac{|k|}{2\pi T}$. We find that the hydrodynamic dispersion relations pass through pole-skipping points $(\mathfrak{w}_n, |\mathfrak{k}_n|)$ along the translation invariant direction in the small momentum and frequency regime. In section 3, we consider the axion field in the Lifshitz black hole with hyperscaling violating factor. The locations of lower half-plane pole-skipping points are the same at negative integer (imaginary) Matsubara frequencies. The hydrodynamic dispersion relation also fits the pole-skipping points well in the small k limit in this section.

In section 4, we calculate the pole-skipping points of a scalar field in the background of $\mathrm{AdS}_2 \times \mathbb{R}^{d-1}$. The results from the near horizon analysis of the bulk equation are the same as Green's function outcomes. We all know that Green's function depends on the boundary conditions. For instance, choosing standard quantization makes Green's function different from choosing alternative quantization for a scalar. However, for the pole-skipping points, choosing different quantization will not affect their positions [23]. We also verify the correctness of this conclusion in this section. In section 5, we obtain the "special points" of sound mode and scalar field in the Rindler horizon. There is no boundary condition in Rindler geometry, so it could be difficult to ensure a "pole-skipping" in the corresponding Green's function. Nevertheless, interestingly we can still obtain "special points" from near horizon analysis, which means there are two incoming solutions near the horizon related to the nonunique of Green's function from a holographic point of view.

2 Anisotropic system near Lifshitz points

In this section, we consider the anisotropic spacetime near Lifshitz points and compute the lower half-plane pole-skipping points in the tensor modes, Maxwell vector and Maxwell scalar mode in the probe limit. The form of action is Einstein-Maxwell-Dilaton action given by [29]

$$S = \int d^{3+1}x\sqrt{-g}(R + \mathcal{L}_M). \tag{2.1}$$

The matter Lagrangian is given by

$$\mathcal{L}_M = -\frac{1}{2}(\nabla\varphi)^2 - V(\varphi) - \frac{Y(\varphi)}{2}(\nabla\psi)^2 - \frac{Z(\varphi)}{4}F^2. \tag{2.2}$$

$V(\varphi)$, $Y(\varphi)$ and $Z(\varphi)$ are the scalar potentials that take the following form in the IR $(r \to 0)$ regime

$$V_{IR} = -V_0 e^{\delta\varphi}, \qquad Y_{IR} = e^{\lambda\varphi}, \qquad Z_{IR} = e^{\zeta\varphi}$$

with the dilaton $\varphi = 2\kappa\log(r)$. The matter Lagrangian becomes

$$\mathcal{L}_M = -\frac{1}{2}(\nabla\varphi)^2 + V_0 r^{2\kappa\delta} - \sum_{\alpha=1}^{p}\frac{r^{2\kappa\lambda_\alpha}}{2}(\nabla\psi_\alpha)^2 - \frac{r^{2\kappa\zeta}}{4}F^2, \tag{2.3}$$

where p is the number of axions and $\psi_\alpha = a_\alpha x_\alpha$. The notation a_α is a constant, which is a measure of the anisotropy along the direction of $\alpha\,(\alpha = x, y)$. The critical scaling of the near-horizon region (IR) is holographically realized by a Lifshitz geometry of the form

$$ds^2 = r^\theta\left(-\frac{f(r)dt^2}{r^{2z}} + L^2\frac{dr^2}{f(r)r^2} + \frac{dx^2}{r^{2\phi}} + \frac{dy^2}{r^2}\right), \tag{2.4}$$

where $f(r) = 1 - (\frac{r}{r_+})^{\delta_0}$, and $\delta_0 = 1 + \phi + z - \theta$, z is the Lifshitz scaling exponent, and θ is the hyperscaling violating exponent. The anisotropy is expressed in terms of the exponent ϕ that relates momenta between two directions

$$|k_x| \sim |k_y|^\phi. \tag{2.5}$$

The relationships between characteristic energies and the momenta in two spatial dimensions are given as

$$\begin{aligned}\omega &\sim |k_x|^{z/\phi},\\ \omega &\sim |k_y|^{z}.\end{aligned} \tag{2.6}$$

The Hawking temperature is given by $T = \frac{|\delta_0| r_+^{-z}}{4\pi L}$. The authors in [29] derived the hyperscaling-violating solutions with an axion ($p = 1$) field in the IR geometry

$$\begin{aligned} z &= \phi, \qquad 2\kappa\delta = -\theta, \qquad \kappa\lambda = -1,\\ 4\kappa^2 &= \theta^2 - 2\theta\phi + 2\phi - 2,\\ L^2 &= (\theta - 2\phi - 1)(\theta - 2\phi)/V_0,\\ a^2 &= \frac{2V_0(1-\phi)}{\theta - 2\phi}.\end{aligned} \tag{2.7}$$

Using the Eddington-Finkelstein (EF) coordinate, we can recast the tortoise coordinate $dr_* = \frac{r^{z-1}}{f(r)} dr$ and $v = t - r_*$ into the metric (2.4) and obtain

$$ds^2 = -r^{\theta-2z} f(r) dv^2 + 2Lr^{\theta-z-1} dvdr + r^{\theta-2\phi} dx^2 + r^{\theta-2} dy^2. \tag{2.8}$$

2.1 Tensor-type perturbations

• **Case one: x-direction (a=0).** Firstly, we consider the tensor type of perturbation along the x-direction of the form $\delta h_{xy} = e^{-i\omega v + ik_x x} h_{xy}(r)$. Note $h_{xy} = g_{xx}\delta h^x_y$. We choose $z = \phi = 1$ to make $a = 0$, the equation of motion for h^x_y is given by [29]

$$\partial_\mu \left(\frac{\sqrt{-g}}{\mathcal{N}} \partial^\mu h^x_y \right) = 0. \tag{2.9}$$

The notations of $\mathcal{N}$ is expressed as

$$\mathcal{N}(r) = g_{yy}(r) g^{xx}(r). \tag{2.10}$$

The equation of perturbation becomes

$$h''^x_y + \left(\frac{f'(r)}{f(r)} - \frac{2i\omega L}{f(r)} + \frac{(\theta-2)}{r} \right) h'^x_y - \frac{L}{f(r)} \left(k_x^2 L + i\omega r^{-1}(\theta - 2) \right) h^x_y = 0. \tag{2.11}$$

We use the approximation $f(r) \sim f'(r_+)(r - r_+)$ near horizon $r = r_+$, and expand the field equation near the horizon $r = r_+$

$$h''^x_y + \frac{1 - i\mathfrak{w}}{r - r_+} h'^x_y + \frac{L}{\delta_0} \left(4\mathfrak{k}_x^2 \pi^2 T^2 L r_+ + i2\pi T \mathfrak{w}(\theta - 2) \right) \frac{h^x_y}{r - r_+} = 0, \tag{2.12}$$

where $\mathfrak{w} = \frac{\omega}{2\pi T}$, and $\mathfrak{k}_x = \frac{k_x}{2\pi T}$. For a generic $(\mathfrak{w}, \mathfrak{k}_x)$, the equation has a regular singularity at $r = r_+$. So one can solve it by a power series expansion around $r = r_+$

$$h^y_x(r) = (r - r_+)^\lambda \sum_{p=0}^{\infty} h^y_{xp} (r - r_+)^p. \tag{2.13}$$

At the lowest order, we can obtain the indicial equation $\lambda(\lambda - i\mathfrak{w}) = 0$. The two solutions become

$$\lambda_1 = 0, \qquad \lambda_2 = i\mathfrak{w}. \tag{2.14}$$

One corresponds the incoming mode and another the outgoing mode. If we choose $i\mathfrak{w} = 1$ and appropriate value of $\mathfrak{k}_x$, make the singularity in front of h'^y_x and h^y_x terms vanishing. We call it a "pole-skipping" point. The regular singularity at $r = r_+$ becomes a regular point at this special point. We take the coefficients $(1 - i\mathfrak{w})$ and $\Big(4\mathfrak{k}_x^2\pi^2T^2Lr_+ + i2\pi T\mathfrak{w}(\theta - 2)\Big)$ to be vanishing. We then obtain the location of the special point in the h^y_x field equation

$$\begin{aligned}\mathfrak{w}_{\star 1} &= -i,\\ \mathfrak{k}^2_{x\star 1} &= \frac{2(2-\theta)}{|\delta_0|}.\end{aligned} \tag{2.15}$$

When $\theta = 0$ and $L^2 = 1$, the metric (2.4) recovers the black brane solution in AdS_4. The pole-skipping point becomes

$$\mathfrak{w}_\star = -i, \qquad \mathfrak{k}^2_{x\star} = \frac{4}{3}. \tag{2.16}$$

This result is the same as (1.7e) in ref. [14].

From (2.15), two solutions in (2.14) become

$$\lambda_1 = 0, \qquad \lambda_2 = 1. \tag{2.17}$$

So that (2.13) can be written as a Taylor series, the special point above is $(\omega_1 = -i2\pi T, k_1)$. We can extend the pole-skipping phenomenon at higher Matsubara frequencies $\omega_n = -i2\pi Tn$ by using the method given in [18]. Now we repeat this process and calculate the special points (ω_n, k_n). Firstly, we expand $h^y_x(r)$ with a Taylor series

$$h^y_x(r) = \sum_{p=0}^{\infty} h^y_{xp}(r - r_+)^p = h^y_{x0} + h^y_{x1}(r - r_+) + h^y_{x2}(r - r_+)^2 + \dots. \tag{2.18}$$

We insert (2.18) into (2.11) and expand the axion equation of motion in powers of $(r - r_+)$. Then, a series of perturbed equation in the order of $(r - r_+)$ can be denoted as

$$S = \sum_{p=0}^{\infty} S_p(r - r_+)^p = S_0 + S_1(r - r_+) + S_2(r - r_+)^2 + \dots. \tag{2.19}$$

We write down the first few equations $S_p = 0$ in the expansion of (2.19)

$$\begin{aligned}0 &= M_{11}(\omega, k^2)h^y_{x0} + (2\pi T - i\omega)h^y_{x1},\\ 0 &= M_{21}(\omega, k^2)h^y_{x0} + M_{22}(\omega, k^2)h^y_{x1} + (4\pi T - i\omega)h^y_{x2},\\ 0 &= M_{31}(\omega, k^2)h^y_{x0} + M_{32}(\omega, k^2)h^y_{x1} + M_{33}(\omega, k^2)h^y_{x2} + (6\pi T - i\omega)h^y_{x3}.\end{aligned} \tag{2.20}$$

To find an incoming solution, we should solve a set of linear equations of the form

$$\mathcal{M}^{(n)}(\omega, k^2)\cdot h^y_x \equiv \begin{pmatrix} M_{11} & (2\pi T - i\omega) & 0 & 0 & \dots \\ M_{21} & M_{22} & (4\pi T - i\omega) & 0 & \dots \\ M_{31} & M_{32} & M_{33} & (6\pi T - i\omega) & \dots \\ \dots & \dots & \dots & \dots & \dots \end{pmatrix} \begin{pmatrix} h^y_{x0} \\ h^y_{x1} \\ h^y_{x2} \\ \dots \end{pmatrix} = 0. \tag{2.21}$$

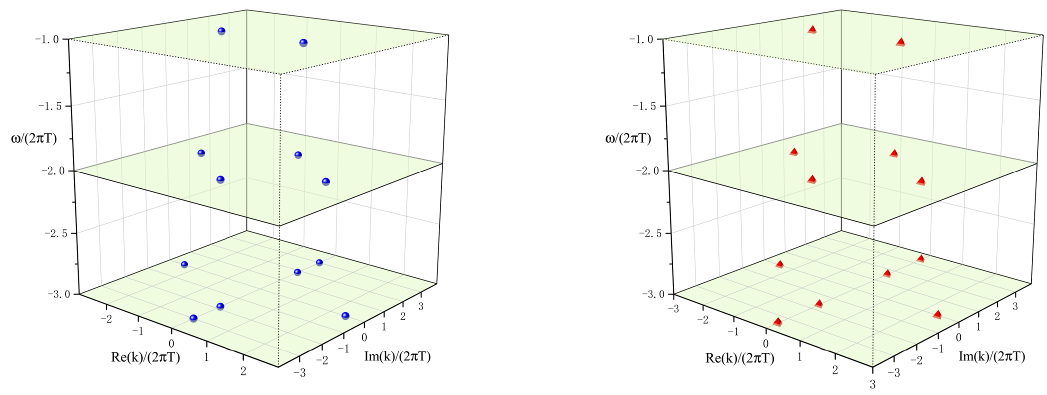

(a) (b)

Figure 1. The first three order pole-skipping points of tensor mode h_x^y along the x-direction in anisotropic system near Lifshitz points when $a = 0$. (a) $\theta = 0$, $z = \phi = 1$; (b) $\theta = -3$, $z = \phi = 1$.

The locations of special points (ω_n, k_n) can be easily extracted from the determinant of the $(n \times n)$ matrix $\mathcal{M}^{(n)}(\omega, k^2)$ constructed by the first n equations

$$\omega_n = -i2\pi T n, \qquad k^2 = k_n^2, \qquad \det\mathcal{M}^{(n)}(\omega, k^2) = 0. \tag{2.22}$$

Therefore, we obtain

$$\begin{aligned}
\mathfrak{w}_{\star 2} &= -2i, \\
\mathfrak{k}^2_{x\star 2,1} &= \frac{4\pi T L\left(2-\theta\right) + r_+ f''\left(r_+\right) - \sqrt{16\pi^2 T^2 L^2\left(12 - 8\theta + \theta^2\right) + 8\pi T L r_+\left(\theta - 2\right) f''\left(r_+\right) + r_+^2 f''^2\left(r_+\right)}}{8\pi^2 T^2 L^2 r_+}, \\
\mathfrak{k}^2_{x\star 2,2} &= \frac{4\pi T L\left(2-\theta\right) + r_+ f''\left(r_+\right) + \sqrt{16\pi^2 T^2 L^2\left(12 - 8\theta + \theta^2\right) + 8\pi T L r_+\left(\theta - 2\right) f''\left(r_+\right) + r_+^2 f''^2\left(r_+\right)}}{8\pi^2 T^2 L^2 r_+}.
\end{aligned} \tag{2.23}$$

At these locations, any value of h_{x0}^y and h_{xn}^y satisfies the equation (2.11); there are two independent free parameters h_{x0}^y and h_{xn}^y in the general series solution (2.18) to this equation. The general ingoing solution to the equation of motion (2.11) is not unique at Matsubara frequencies $\omega_n = -i2\pi T n$. The first few elements of this matrix have been shown in appendix A.1.1. Then we calculate the first three order pole-skipping points and plot them in figure 1.

(a) $\theta = 0$, $\phi = z = 1$

$$\begin{aligned}
&\mathfrak{w}_{\star 1} = -i, \qquad \mathfrak{k}_{x\star 1} = \pm 1.155; \\
&\mathfrak{w}_{\star 2} = -2i, \qquad \mathfrak{k}_{x\star 2,1} = \pm 1.807, \qquad \mathfrak{k}_{x\star 2,2} = \pm 1.807i; \\
&\mathfrak{w}_{\star 3} = -3i, \qquad \mathfrak{k}_{x\star 3,1} = \pm 2.402, \qquad \mathfrak{k}_{x\star 3,2} = \pm 1.849i, \qquad \mathfrak{k}_{x\star 3,3} = \pm 3.002i.
\end{aligned} \tag{2.24}$$

JHEP06(2021)165

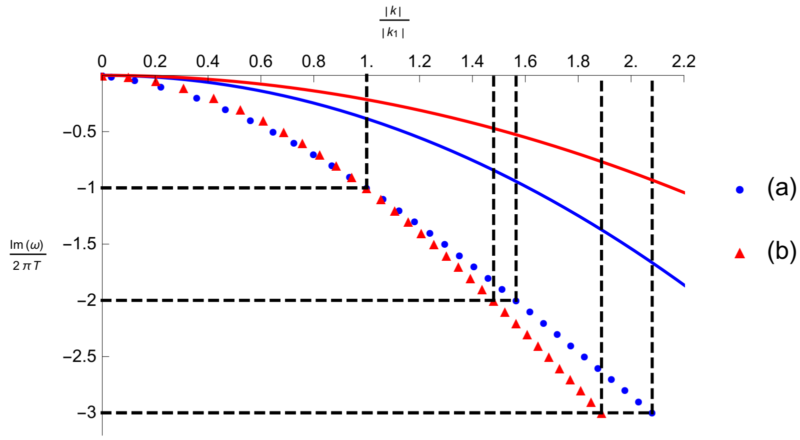

Figure 2. Solid lines show the diffusive hydrodynamic dispersion relation (2.26). The intersections of the dashed lines correspond to the first three order pole-skipping points of tensor mode h_x^y along the x-direction in the anisotropic system near Lifshitz points when $a = 0$. Blue dots and red triangles show the curve fitting of pole-skipping points of the data which we set (a) $z = \phi = 1$, $\theta = 0$; (b) $z = \phi = 1$, $\theta = -3$.

(b) $\theta = -3$, $\phi = z = 1$

$$\begin{aligned}
&\mathfrak{w}_{\star 1} = -i, && \mathfrak{k}_{x\star 1} = \pm 1.291; \\
&\mathfrak{w}_{\star 2} = -2i, && \mathfrak{k}_{x\star 2,1} = \pm 1.911, && \mathfrak{k}_{x\star 2,2} = \pm 1.911i; \\
&\mathfrak{w}_{\star 3} = -3i, && \mathfrak{k}_{x\star 3,1} = \pm 1.633i, && \mathfrak{k}_{x\star 3,2} = \pm 2.438, && \mathfrak{k}_{x\star 3,3} = \pm 3.407i.
\end{aligned} \tag{2.25}$$

The transverse momentum Green's function has a hydrodynamic pole corresponding to the diffusion of momentum with the small k dispersion relation [27]

$$\omega(k) = -iD_p k^2 + \dots. \tag{2.26}$$

Because $a = 0$, the momentum along the x-direction is without dissipation. So $\frac{\eta_{yxyx}}{s} = \frac{1}{4\pi}\frac{g_{xx}}{g_{yy}}|_{r_+}$ [29]. We obtain the momentum diffusion constant $D_p = \eta/(sT) = 1/(4\pi T)$. We study the complex hydrodynamics in the complex momentum plane. We plot the first three order pole-skipping points of $(\mathfrak{w}_n, |\mathfrak{k}_n|)$ and the hydrodynamic dispersion relation in terms of dimensionless variables $\frac{\omega}{2\pi T}$ and $\frac{|k|}{2\pi T}$ in figure 2. We can see that the dispersion relation $\omega(k)$ of a hydrodynamic mode passes through pole-skipping points when $\omega, k \to 0$.

• **Case two: x-direction ($a \neq 0$).** Now we choose $z = \phi \neq 1$ so that $a \neq 0$. The equation of motion for h_y^x becomes [29]

$$\partial_\mu\left(\frac{\sqrt{-g}}{\mathcal{N}}\partial^\mu h_y^x\right) - \frac{\sqrt{-g}}{\mathcal{N}} m^2 h_y^x = 0. \tag{2.27}$$

The notation of m^2 is expressed as $m^2(r) = a^2 Y(\varphi) g^{xx}(r)$. In this case, the translational symmetry along the x-direction is broken, and the momentum is dissipated at a strength controlled by a. If we drop the mass term m^2, the equation is same as the isotropic one (2.9) discussed in the previous case.

Equation (2.27) can be recast as

$$h''^{x}_{y}+\left(\frac{f'(r)}{f(r)}-\frac{2i\omega Lr^{\phi-1}}{f(r)}+(\theta-4\phi+2)r^{-1}\right)h'^{x}_{y}$$
$$-\frac{L}{f(r)}\left(a^2Lr^{2(\kappa\lambda+\phi)-2}+k_x^2Lr^{2\phi-2}+i\omega r^{\phi-2}(\theta-3\phi+1)\right)h^x_y=0. \tag{2.28}$$

We also use the approximation $f(r)\sim f'(r_+)(r-r_+)$ near the horizon $r=r_+$. We expand the field equation near the horizon $r=r_+$

$$h''^{y}_{x}+\frac{1-i\mathfrak{w}}{r-r_+}h'^{x}_{y}+\frac{L}{\delta_0}\left(a^2Lr^{2(\kappa\lambda+\phi)-1}+4\mathfrak{k}_x^2\pi^2T^2Lr^{2\phi-1}+i2\pi T\mathfrak{w}r^{\phi-1}(\theta-3\phi+1)\right)\frac{h^x_y}{r-r_+}=0. \tag{2.29}$$

We take the value of coefficients $(1-i\mathfrak{w})$ and $\frac{L}{\delta_0}\Big(a^2Lr^{2(\kappa\lambda+\phi)-1}+4\mathfrak{k}_x^2\pi^2T^2Lr^{2\phi-1}+i2\pi T\mathfrak{w}r^{\phi-1}(\theta-3\phi+1)\Big)$ to become 0 and eliminate the singularity in front of h'^{y}_{x} and h^y_x terms. Then, we find the location of the special point

$$\mathfrak{w}_{\star1}=-i,$$
$$\mathfrak{k}^2_{x\star1}=\frac{-2|\delta_0|(\theta-3\phi+1)-4a^2L^2r_+^{2(\kappa\lambda+\phi)}}{|\delta_0|^2}. \tag{2.30}$$

If we set $\phi=1$ to make $a=0$, we can see this result becomes (2.15). We can also evaluate the higher special points

$$\omega_n=-i2\pi Tn,\qquad k^2=k_n^2,\qquad \det\mathcal{M}^{(n)}(\omega,k^2)=0. \tag{2.31}$$

$$\mathfrak{w}_{\star2}=-2i,$$
$$\mathfrak{k}^2_{x\star2,1}=\frac{r_+^{-2\phi}}{8\pi^2T^2L^2}\Big(r_+^2f''(r_+)-2a^2L^2r_+^{2(\kappa\lambda+\phi)}-4\pi TLr_+^{\phi}(\theta-2\phi)-\sqrt{16\pi TL^2r_+^{2\phi}(2a^2Lr_+^{2\kappa\lambda+\phi}\kappa\lambda\;\overline{+\pi T(4+4\theta+\theta^2-20\phi-12\theta\phi+28\phi^2))-8\pi TLr_+^{\phi+2}(4\phi-\theta-2)f''(r_+)+r_+^4f''^2(r_+)}}\Big),$$
$$\mathfrak{k}^2_{x\star2,2}=\frac{r_+^{-2\phi}}{8\pi^2T^2L^2}\Big(r_+^2f''(r_+)-2a^2L^2r_+^{2(\kappa\lambda+\phi)}-4\pi TLr_+^{\phi}(\theta-2\phi)+\sqrt{16\pi TL^2r_+^{2\phi}(2a^2Lr_+^{2\kappa\lambda+\phi}\kappa\lambda\;\overline{+\pi T(4+4\theta+\theta^2-20\phi-12\theta\phi+28\phi^2))-8\pi TLr_+^{\phi+2}(4\phi-\theta-2)f''(r_+)+r_+^4f''^2(r_+)}}\Big). \tag{2.32}$$

The first few elements of this matrix have been shown in appendix A.1.2. Then we calculate the first three order pole-skipping points and plot them in figure 3. We choose the following parameters and obtain $(\mathfrak{w}_\star,\mathfrak{k}_{x\star})$ as follows

(a) $\theta=-1$, $z=\phi=2$ $(a=3.46)$

$$\mathfrak{w}_{\star1}=-i,\qquad \mathfrak{k}_{x\star1}=\pm0.816;$$
$$\mathfrak{w}_{\star2}=-2i,\qquad \mathfrak{k}_{x\star2,1}=\pm1.758,\qquad \mathfrak{k}_{x\star2,2}=\pm2.400i;$$
$$\mathfrak{w}_{\star3}=-3i,\qquad \mathfrak{k}_{x\star3,1}=\pm2.462,\qquad \mathfrak{k}_{x\star3,2}=\pm2.506i,\qquad \mathfrak{k}_{x\star3,3}=\pm3.713i. \tag{2.33}$$

JHEP06(2021)165

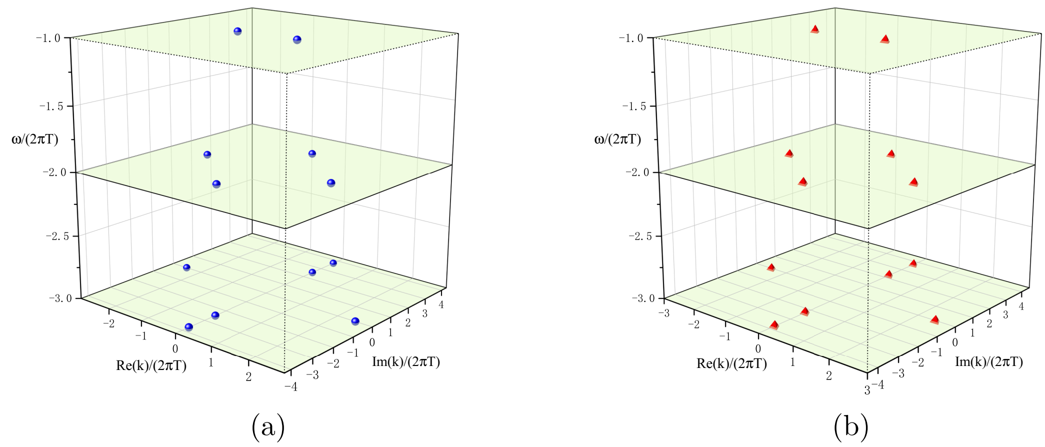

Figure 3. The first three order pole-skipping points of tensor mode h_x^y along the x-direction in the anisotropic system near Lifshitz points when $a \neq 0$. (a) $\theta = -1$, $z = \phi = 2$ ($a = 3.46$); (b) $\theta = -3$, $z = \phi = 2$ ($a = 4$).

(b) $\theta = -3$, $\phi = z = 2$ $(a = 4)$

$$\begin{aligned} &\mathfrak{w}_{\star 1} = -i, && \mathfrak{k}_{x\star 1} = \pm 1; \\ &\mathfrak{w}_{\star 2} = -2i, && \mathfrak{k}_{x\star 2,1} = \pm 1.833, \quad \mathfrak{k}_{x\star 2,2} = \pm 2.345i; \\ &\mathfrak{w}_{\star 3} = -3i, && \mathfrak{k}_{x\star 3,1} = \pm 2.270i, \quad \mathfrak{k}_{x\star 3,2} = \pm 2.478, \quad \mathfrak{k}_{x\star 3,3} = \pm 3.741i. \end{aligned} \tag{2.34}$$

2.2 Sound modes

The sound modes of the metric perturbation are given by

$$\begin{aligned} h_{vv} &= e^{-i\omega v + ik_x x} h_{vv}(r), \qquad h_{vx} = e^{-i\omega v + ik_x x} h_{vx}(r), \\ h_{xx} &= e^{-i\omega v + ik_x x} h_{xx}(r), \qquad h_{yy} = e^{-i\omega v + ik_x x} h_{yy}(r). \end{aligned} \tag{2.35}$$

Substitute (2.35) into the linearized Einstein equation

$$R_{\mu\nu} - \frac{1}{2} R g_{\mu\nu} = -\frac{1}{\sqrt{-g}} \frac{\delta(\sqrt{-g}\mathcal{L}_M)}{\delta g^{\mu\nu}}, \tag{2.36}$$

where $\mathcal{L}_M$ is given by equation (2.2). We obtain the vv component near the horizon r_+

$$L\left(2kr_+^{2\phi} h_{tx} + r_+^{2\phi}\omega h_{xx} + r_+^2 \omega h_{yy}\right)(\omega - 2i\pi T) + h_{tt}\left(Lk_x^2 r_+^{2\phi} - Lr_+^{\theta}\mathcal{L}_M + r_+^{\phi}(\phi - \theta + 1)(i\omega - 4\pi T)\right). \tag{2.37}$$

The upper-half ω-plane of the pole-skipping point is located at

$$\omega_\star = i2\pi T, \qquad k_{x\star}^2 = \frac{6\pi T(\phi - \theta + 1)r_+^{-\phi}}{L} + \mathcal{L}_M r_+^{\theta - 2\phi}. \tag{2.38}$$

The Lyapunov exponent and butterfly velocity can be calculated by equation (1.3)

$$\lambda_L = 2\pi T, \qquad v_B^2 = \frac{|\omega|^2}{|k_x^2|} = \frac{4\pi^2 T^2 L^2 r^{4\phi}}{\left(L\mathcal{L}_M r_+^{\theta} + 6\pi T(\phi - \theta + 1) r_+^{\phi}\right)^2}. \tag{2.39}$$

JHEP06(2021)165

2.3 Maxwell field

2.3.1 Maxwell vector mode

We consider the Maxwell vector perturbation $A_y = a_y e^{-i\omega v + i k_x x}$ in the probe limit. The Maxwell vector equation is written as [29]

$$\partial_\nu \left(\sqrt{-g} Z(\varphi) F^{\mu\nu}\right) = 0. \tag{2.40}$$

In the region of IR, $Z(\varphi)$ equals $r^{2\kappa\zeta}$. We substitute it into (2.40) and obtain

$$\begin{aligned} &A_y'' + \left(\frac{f'(r)}{f(r)} - \frac{2i\omega r^{z-1}}{f(r)} + (2 - z + 2\kappa\zeta - \phi) r^{-1}\right) A_y' \\ &- \frac{1}{f(r)}\left(k_x^2 r^{2\phi-2} + i\omega(1 + 2\kappa\zeta - \phi) r^{z-2}\right) A_y = 0. \end{aligned} \tag{2.41}$$

Using the approximation $f(r) \sim f'(r_+)(r - r_+)$ near horizon $r = r_+$, we expand the field equation near horizon $r = r_+$

$$A_y'' + \frac{1 - i\mathfrak{w}}{r - r_+} A_y' - \frac{1}{|\delta_0|}\left(4\mathfrak{k}_x^2 \pi^2 T^2 r^{2\phi-2} + i2\pi T \mathfrak{w}(1 + 2\kappa\zeta - \phi) r^{z-2}\right)\Big|_{r=r_+} \frac{A_y}{r - r_+} = 0. \tag{2.42}$$

We take the value of terms $(1 - i\mathfrak{w})$ and $\frac{1}{|\delta_0|}\left(4\mathfrak{k}_x^2 \pi^2 T^2 r^{2\phi-2} + i2\pi T\mathfrak{w}(1 + 2\kappa\zeta - \phi) r^{z-2}\right)\Big|_{r=r_+}$ to be 0 and eliminate the singularity in front of A_y' and A_y terms. The location of the special point about Maxwell vector mode is given as

$$\begin{aligned} \mathfrak{w}_\star &= -i, \\ \mathfrak{k}_{x\star}^2 &= \frac{2(\phi - 2\kappa\zeta - 1) r_+^{2z-2\phi-1}}{|\delta_0|}. \end{aligned} \tag{2.43}$$

When $z = \phi = 1$ and $\theta = 0$, the parameter $\kappa = 0$ from equation (2.7). The metric (2.4) recovers the black brane solution in AdS_4. The pole-skipping point becomes

$$\mathfrak{w}_\star = -i, \qquad \mathfrak{k}_{x\star}^2 = 0. \tag{2.44}$$

This result is the same as (1.7b) in ref. [14] by choosing horizon radius $r_+ = 1$. We also evaluate the higher special points

$$\omega_n = -i2\pi T n, \qquad k^2 = k_n^2, \qquad \det \mathcal{M}^{(n)}\left(\omega, k^2\right) = 0. \tag{2.45}$$

The first few elements of this matrix have been shown in appendix A.1.3. Then we calculate the first three order pole-skipping points and plot them in figure 4.

(a) $z = \phi = 1,\ \zeta = -1,\ \theta = 9$

$$\begin{aligned} &\mathfrak{w}_{\star 1} = -i, && \mathfrak{k}_{x\star 1} = \pm 1.627; \\ &\mathfrak{w}_{\star 2} = -2i, && \mathfrak{k}_{x\star 2,1} = \pm 2.238i, \quad \mathfrak{k}_{x\star 2,2} = \pm 2.374; \\ &\mathfrak{w}_{\star 3} = -3i, && \mathfrak{k}_{x\star 3,1} = \pm 2.879i, \quad \mathfrak{k}_{x\star 3,2} = \pm 2.969, \quad \mathfrak{k}_{x\star 3,3} = \pm 3.356i. \end{aligned} \tag{2.46}$$

JHEP06(2021)165

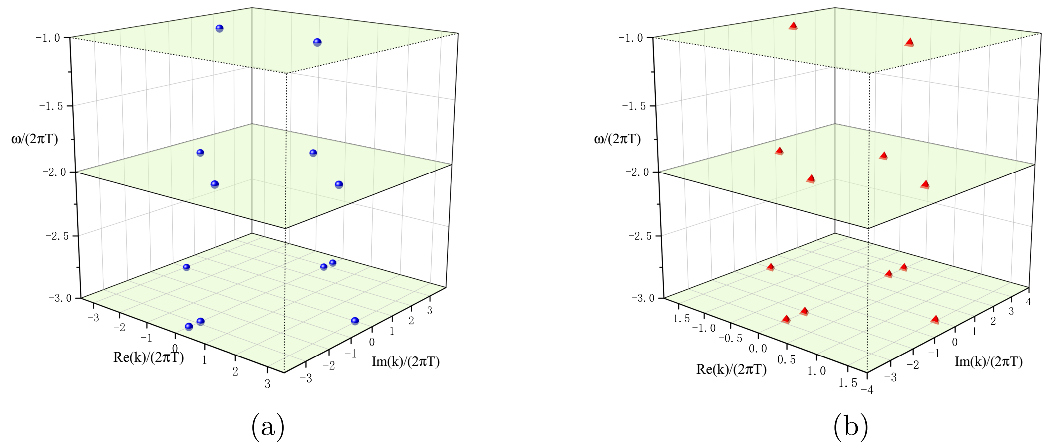

Figure 4. The first three order pole-skipping points of Maxwell vector mode A_y in the anisotropic system near Lifshitz points. (a) $\theta = 9$, $\zeta = -1$, $z = \phi = 1$; (b) $\theta = 4$, $\zeta = -1$, $z = \phi = -1$.

(b) $z = \phi = -1$, $\zeta = -1$, $\theta = 4$

$$\begin{aligned} &\mathfrak{w}_{\star 1} = -i, && \mathfrak{k}_{x\star 1} = \pm 0.994; \\ &\mathfrak{w}_{\star 2} = -2i, && \mathfrak{k}_{x\star 2,1} = \pm 1.285, \quad \mathfrak{k}_{x\star 2,2} = \pm 1.695i; \\ &\mathfrak{w}_{\star 3} = -3i, && \mathfrak{k}_{x\star 3,1} = \pm 1.494, \quad \mathfrak{k}_{x\star 3,2} = \pm 2.028i, \quad \mathfrak{k}_{x\star 3,3} = \pm 2.820i. \end{aligned} \tag{2.47}$$

The hydrodynamic pole corresponding to the diffusion of charge with the small-k dispersion relation is given by [27]

$$\omega(k) = -iD_c k^2 + \dots, \tag{2.48}$$

where the charge diffusion constant is given by $D_{c,\alpha} = -\frac{L}{\Delta_\chi}\frac{r^{\theta-z}}{g_{\alpha\alpha}(r)}|_{r_+}$, and Δ_χ is the scaling dimension of the charge susceptibility [29]. The momenta k_n are complex numbers, so we perform the complex hydrodynamic analyses. We plot the first three order pole-skipping points of $(\mathfrak{w}_n, |\mathfrak{k}_n|)$ and the hydrodynamic dispersion relation in terms of dimensionless variables $\frac{\omega}{2\pi T}$ and $\frac{|k|}{2\pi T}$ in figure 5. They fit well within the small k limit. So this is a general conclusion in which the hydrodynamic pole corresponds to the diffusion of both momentum and charge.

2.3.2 Maxwell scalar mode

The gauge-invariant variables of the Maxwell scalar mode are

$$\begin{aligned} \mathfrak{A}_t &= A_t + \frac{\omega}{k_x}A_x, \\ \mathfrak{A}_r &= A_r - \frac{1}{ik_x}A_x' \end{aligned} \tag{2.49}$$

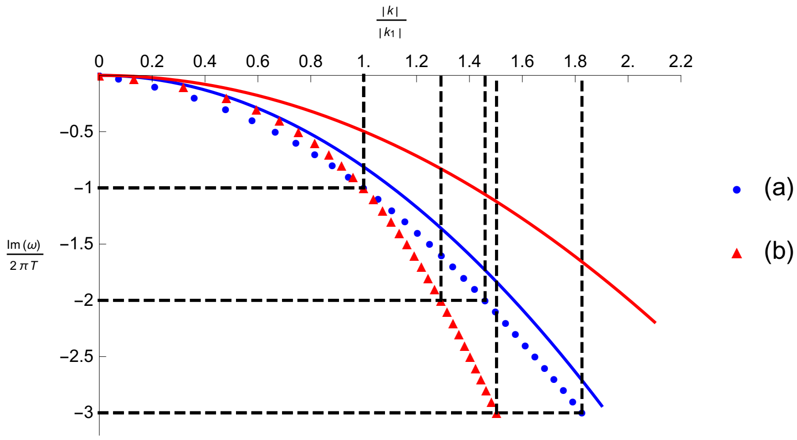

Figure 5. Solid lines show the diffusive hydrodynamic dispersion relation (2.48). The intersections of the dashed lines correspond to the first three order pole-skipping points of Maxwell vector mode A_y in the anisotropic system near Lifshitz points. Blue dots and red triangles show the curve fitting of pole-skipping points represent the data which we choose (a) $\theta = 9$, $\zeta = -1$, $z = \phi = 1$; (b) $\theta = 4$, $\zeta = -1$, $z = \phi = -1$.

with $A_x = a_x e^{-i\omega v + ik_x x}$. Combining the Maxwell scalar equations by gauge-invariant variables, we obtain

$$\begin{aligned}\mathfrak{A}_r' &+ \left(\frac{f'(r)}{f(r)} - \frac{2i\omega L r^{z-1}}{f(r)} - \frac{k^2 L r^{2\phi-z-1}}{i\omega} - (z - 2\kappa\zeta - \phi)\, r^{-1}\right)\mathfrak{A}_r \\ &+ \frac{L}{f(r)}\left((2\kappa\zeta + \phi - 1)\, r^{z-2} - \frac{k_x^2 r^{2\phi-z-2}}{i\omega}\right)\mathfrak{A}_t = 0. \end{aligned} \tag{2.50}$$

We use the approximation $f(r) \sim f'(r)(r - r_+)$ near the horizon radius $r = r_+$. Then the field equation near $r = r_+$ is given by

$$\mathfrak{A}_r' + \frac{1 - i\mathfrak{w}}{r - r_+}\mathfrak{A}_r + \frac{L}{f'(r)}\left((2\kappa\zeta + \phi - 1)\, r^{z-2} - \frac{2\pi T \mathfrak{k}_x^2 r^{2\phi-z-2}}{i\mathfrak{w}}\right)\bigg|_{r=r_+} \frac{\mathfrak{A}_t}{r - r_+} = 0. \tag{2.51}$$

We obtain the first order special point about Maxwell scalar mode by taking the terms $(1 - i\mathfrak{w})$ and $\frac{L}{f'(r)}\left((2\kappa\zeta + \phi - 1) r^{z-2} - \frac{2\pi T \mathfrak{k}_x^2 r^{2\phi-z-2}}{i\mathfrak{w}}\right)\bigg|_{r=r_+}$ vanish.

$$\begin{aligned}\mathfrak{w}_\star &= -i, \\ \mathfrak{k}_{x\star}^2 &= \frac{2(\phi + 2\kappa\zeta - 1) r_+^{3z-2\phi-1}}{|\delta_0|}.\end{aligned} \tag{2.52}$$

When $z = \phi = 1$ and $\theta = 0$, the result recovers the Maxwell scalar pole-skipping point corresponding to (1.7c) in ref. [14]

$$\mathfrak{w}_\star = -i, \quad \mathfrak{k}_{x\star}^2 = 0. \tag{2.53}$$

3 Lifshitz black hole with linear axion fields and hyperscaling violating factor

In this section, we consider the background of Lifshitz black holes with linear axion fields and hyperscaling violating factor. We will compute the lower half-plane pole-skipping points in the axion field. The general action is given by [30–33]

$$S = \frac{1}{16\pi G_{d+2}} \int d^{d+2}x\sqrt{-g}[R + V(\phi) - \frac{1}{2}(\partial\phi)^2 - \frac{1}{4}\sum_{\mathrm{i}=1}^{n} Z_{\mathrm{i}}(\phi)F_{(\mathrm{i})}^2 - \frac{1}{2}\sum_{\mathrm{j}}^{d} Y(\phi)(\partial\chi_{\mathrm{j}})^2], \tag{3.1}$$

where $Z_{\mathrm{i}}(\phi) = e^{\lambda_{\mathrm{i}}\phi}$ and $Y(\phi) = e^{-\lambda_2\phi}$, R is the Ricci scalar, χ_{i} is d-massless linear axions. $F_{rt}^{(1)}$ is an auxiliary gauge field, and $F_{rt}^{(2)}$ is a gauge field analogous to a Maxwell field. The black hole solution is given by [30, 31, 33]

$$ds^2 = r^{-\frac{2\theta}{d}}\left(-r^{2z}f(r)dt^2 + \frac{dr^2}{r^2 f(r)} + r^2 d\vec{x}_d^2\right), \tag{3.2}$$

with the notations

$$\begin{aligned}
f(r) &= 1 - \frac{m}{r^{d+z-\theta}} + \frac{Q^2}{r^{2(d+z-\theta-1)}} - \frac{\beta^2}{r^{2z-2\theta/d}},\\
F_{(1)rt} &= Q_1\sqrt{2(z-1)(z-d-\theta)}r^{d+z-\theta-1},\\
F_{(2)rt} &= Q_2\sqrt{2(d-\theta)(z-\theta+d-2)}r^{-(d+z-\theta-1)},\\
\lambda_1 &= -\frac{2d-2\theta+\frac{2\theta}{d}}{\sqrt{2(d-\theta)(z-1-\theta/d)}},\\
\lambda_2 &= \sqrt{2\frac{z-1-\theta/d}{d-\theta}},\\
e^{\phi} &= r^{\sqrt{2(d-\theta)(z-1-\theta/d)}},\\
V(\phi) &= (z+d-\theta-1)(z+d-\theta)r^{2\theta/d},\\
\chi_{\mathrm{i}} &= \beta x^a, \qquad \mathrm{i} \in \{1, d\}, \quad a \in \{x, y\ldots\}.
\end{aligned} \tag{3.3}$$

The mass m in terms of r_H is

$$m = r_H^{d+z-\theta} + Q_2^2 r_H^{2-d-z-\theta} - \beta^2 r_H^{d-z-\theta+2\theta/d}. \tag{3.4}$$

The Hawking temperature is given by

$$T = \frac{r_H^{z+1}f'(r_H)}{4\pi} = \frac{m(2+z-\theta)r_H^{\theta-2} + \beta^2(2z-\theta)r_H^{\theta-2} + 2Q^2(\theta-z-1)r_H^{2\theta-z-2}}{4\pi}. \tag{3.5}$$

We consider the $d = 2$ dimensional case in the following. For simplicity of calculation, we use the Eddington-Finkelstein (EF) coordinates. By putting the tortoise coordinate $dr_* = \frac{1}{r^{z+1}f(r)}dr$ and $v = t - r_*$ into the metric (3.2), we obtain

$$ds^2 = r^{2z-\theta}f(r)dv^2 + 2r^{z-\theta-1}dvdr + r^{2-\theta}d\vec{x}_2^2. \tag{3.6}$$

We want to find lower half-plane pole-skipping points located at Matsubara frequencies $\mathfrak{w}_n := \frac{\omega_n}{2\pi T} = -in$ in this background. So we only consider the linear perturbation of axion field $\chi(r) = \beta x + \bar{\chi}(r)e^{-i\omega t + ik_x x}$ in this section. We choose the parameter $\beta = 0.1$, which is small enough in the following, so that we can take the equation of motion of the axion field as a probe. Then we write down the equation of motion for axions [31, 33, 34]

$$\nabla_\mu(Y(\phi)\nabla^\mu\chi) = 0. \tag{3.7}$$

We obtain

$$\begin{aligned} &\chi''(r) + \left(\frac{f'(r)}{f(r)} - \frac{2i\omega r^{-z-1}}{f(r)} + (\theta - z - 3 + \delta)\, r^{-1}\right)\chi'(r) \\ &+ \frac{1}{f(r)}\left(i\omega(\theta - 2 + \delta)r^{-z-2} - k_x^2 r^{-4}\right)\chi(r) = 0, \end{aligned} \tag{3.8}$$

where the prime symbol denotes derivative with respect to r with the notation $\delta = |2 - 2z + \theta|$. We use the approximation $f(r) \sim f'(r_H)(r - r_H)$ near horizon $r = r_H$. The field equation near $r = r_H$ of $\chi(r)$ is given by

$$\begin{aligned} &\chi'' + \frac{1}{f'(r_H)}\left(f'(r_H) - 2i\omega r_H^{-z-1} + f'(r_H)(r - r_H)(\theta - z - 3 + \delta)\, r_H^{-1}\right)\frac{\chi'}{(r - r_H)} \\ &+ \frac{1}{f'(r_H)}\left(i\omega(\theta - 2 + \delta)r_H^{-z-2} - k_x^2 r_H^{-4}\right)\frac{\chi}{(r - r_H)} = 0. \end{aligned} \tag{3.9}$$

By defining $\mathfrak{w} = \frac{\omega}{2\pi T}$ and $\mathfrak{k}_x = \frac{k_x}{2\pi T}$, the equation (3.9) becomes

$$\chi'' + \frac{1 - i\mathfrak{w}}{r - r_H}\chi' - \left(\frac{i\mathfrak{w}}{2} r_H^{-1} - 4\mathfrak{k}_x^2\pi^2 T^2 r_H^{-4}\right)\frac{\chi}{r - r_H} = 0. \tag{3.10}$$

For a generic $(\mathfrak{w}, \mathfrak{k}_x)$, the equation has a regular singularity at $r = r_H$. So we can also solve it by a power series around $r = r_H$

$$\chi(r) = (r - r_H)^\lambda \sum_{p=0}^{\infty} \chi_p (r - r_H)^p. \tag{3.11}$$

At the lowest order, we can obtain the same indicial equation $\lambda(\lambda - i\mathfrak{w}) = 0$ as the result of section 2. The two solutions are also

$$\lambda_1 = 0, \qquad \lambda_2 = i\mathfrak{w}. \tag{3.12}$$

We choose $i\mathfrak{w} = 1$ and the appropriate value of $\mathfrak{k}_x$ to make the singularity in front of χ' and χ terms vanishing. The terms $(1 - i\mathfrak{w})$ and $\left(\frac{i\mathfrak{w}}{2} r_H^{-1} - 4\mathfrak{k}_x^2\pi^2 T^2 r_H^{-4}\right)$ become 0. Then we find the location of the special point

$$\begin{aligned} &\mathfrak{w}_\star = -i, \\ &\mathfrak{k}_{x\star}^2 = \frac{2(\theta - 2 + \delta)}{-2Q^2(1 + z - \theta)r_H^{2\theta-4} - \beta^2(\theta - 2z)r_H^{\theta-2} - m(\theta - z - 2)r_H^{\theta+z-4}}. \end{aligned} \tag{3.13}$$

When $\theta = 0$, $z = 1$, $Q = 0$ and $\beta = 0$, the metric (3.2) recovers the black brane solution in AdS_4. The pole-skipping point then becomes

$$\mathfrak{w}_\star = -i, \qquad \mathfrak{k}_{x\star}^2 = -\frac{4}{3}. \tag{3.14}$$

This result is the same as (1.7a) in ref. [14]. We extend the pole-skipping phenomenon at higher Matsubara frequencies $\omega_n = -i2\pi T n$, and the method has been shown in section 2. We expand $\chi(r)$ in a Taylor series

$$\chi(r) = \sum_{p=0}^{\infty} \chi_p (r - r_H)^p = \chi_0 + \chi_1 (r - r_H) + \dots . \tag{3.15}$$

We insert (3.15) into (3.8), and write down a series of the perturbed equation in the order of $(r - r_H)$

$$S = \sum_{p=0}^{\infty} S_p (r - r_H)^p = S_0 + S_1 (r - r_H)^p + \dots . \tag{3.16}$$

We spell out the first few equations $S_p = 0$ in the expansion of (3.16)

$$\begin{aligned}
0 &= M_{11}\left(\omega, k^2\right)\chi_0 + (2\pi T - i\omega)\,\chi_1, \\
0 &= M_{21}\left(\omega, k^2\right)\chi_0 + M_{22}\left(\omega, k^2\right)\chi_1 + (4\pi T - i\omega)\,\chi_2, \\
0 &= M_{31}\left(\omega, k^2\right)\chi_0 + M_{32}\left(\omega, k^2\right)\chi_1 + M_{33}\left(\omega, k^2\right)\chi_2 + (6\pi T - i\omega)\,\chi_3.
\end{aligned} \tag{3.17}$$

To find an incoming solution, we should solve a set of linear equations of form

$$\mathcal{M}^{(n)}(\omega, k^2)\cdot\chi \equiv \begin{pmatrix} M_{11} & (2\pi T - i\omega) & 0 & 0 & \dots \\ M_{21} & M_{22} & (4\pi T - i\omega) & 0 & \dots \\ M_{31} & M_{32} & M_{33} & (6\pi T - i\omega) & \dots \\ \dots & \dots & \dots & \dots & \dots \end{pmatrix} \begin{pmatrix} \chi_0 \\ \chi_1 \\ \chi_2 \\ \dots \end{pmatrix} = 0 \tag{3.18}$$

The locations of the special points (ω_n, k_n) can be easily extracted from the determinant of the $(n \times n)$ matrix $\mathcal{M}^{(n)}(\omega, k^2)$ constructed by the first n equations:

$$\omega_n = -i2\pi T n, \qquad k^2 = k_n^2, \qquad \det\mathcal{M}^{(n)}(\omega, k^2) = 0. \tag{3.19}$$

The first few elements of this matrix have shown in appendix A.2. The first three order pole-skipping points are shown in figure 6. We choose the charges $Q_1 = Q_2 = 1$ and obtain $(\mathfrak{w}_\star, \mathfrak{k}_{x\star})$ as follows.

(a) $z = 2$, $\theta = 3$

$$\begin{aligned}
&\mathfrak{w}_{\star 1} = -i, && \mathfrak{k}_{\star 1} = \pm 1.414; \\
&\mathfrak{w}_{\star 1} = -2i, && \mathfrak{k}_{\star 2,1} = \pm 2.000, && \mathfrak{k}_{\star 2,2} = \pm 2.449; \\
&\mathfrak{w}_{\star 1} = -3i, && \mathfrak{k}_{\star 3,1} = \pm 2.449, && \mathfrak{k}_{\star 3,2} = \pm 2.922, && \mathfrak{k}_{\star 3,3} = \pm 3.932.
\end{aligned} \tag{3.20}$$

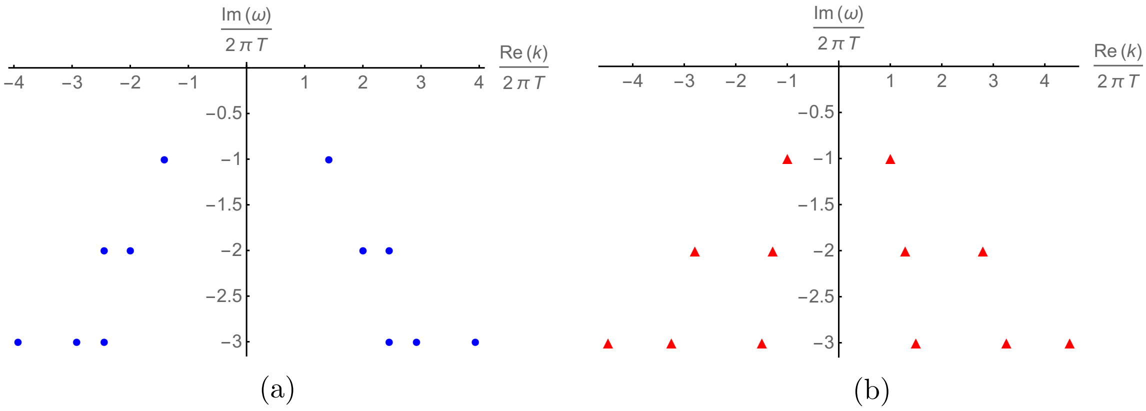

Figure 6. The first three order pole-skipping points of axion field $\chi(r)$ in Lifshitz spacetime with linear axion fields and hyperscaling violating factor. (a) $z = 2$, $\theta = 3$; (b) $z = 2.5$, $\theta = 2.5$.

(b) $z = 2.5$, $\theta = 3$

$$\begin{aligned}
&\mathfrak{w}_{\star 1} = -i, && \mathfrak{k}_{\star 1} = \pm 0.999; \\
&\mathfrak{w}_{\star 2} = -2i, && \mathfrak{k}_{\star 2,1} = \pm 1.286, && \mathfrak{k}_{\star 2,2} = \pm 2.795; \\
&\mathfrak{w}_{\star 3} = -3i, && \mathfrak{k}_{\star 3,1} = \pm 1.495, && \mathfrak{k}_{\star 3,2} = \pm 3.252, && \mathfrak{k}_{\star 3,3} = \pm 4.480.
\end{aligned} \tag{3.21}$$

We depict the first three order pole-skipping points and hydrodynamic dispersion relation (2.26) in figure 7. They fit well at small ω and k. The first few elements of this matrix have shown in appendix A.3. We plot these points in figure 8. The result of the first order pole-skipping point is the same as (1.7a) in ref. [14].

4 $\mathrm{AdS}_2 \times \mathbb{R}^{d-1}$ geometry

We are interested in the locations of pole-skipping points in $\mathrm{AdS}_2 \times \mathbb{R}^{d-1}$. We want to see if different boundary conditions have an impact on the location of pole-skipping points. The $\mathrm{AdS}_2 \times \mathbb{R}^{d-1}$ geometry is given by [35].

$$ds^2 = \frac{R_2^2}{\zeta^2}\left(-\left(1-\frac{\zeta^2}{\zeta_0^2}\right)d\tau^2 + \frac{d\zeta^2}{1-\frac{\zeta^2}{\zeta_0^2}}\right) + \frac{r_*^2}{R^2}dx^2 + \frac{r_*^2}{R^2}dy^2, \tag{4.1}$$

where a temperature $T = \frac{1}{2\pi\zeta_0}$, $Q \equiv \sqrt{\frac{d}{d-2}}r_*^{d-1}$ and r_* is a length scale of charge Q, which has the dimension of $[L]^{d-1}$. Finite value parameter ζ_0 is the horizon radius. R_2 is the curvature radius of AdS_2, and R is the curvature radius of AdS. Using the Eddington-Finkelstein (EF) coordinates, the metric (4.1) becomes

$$ds^2 = -\frac{R_2^2}{\zeta^2}\left(\left(1-\frac{\zeta^2}{\zeta_0^2}\right)dv^2 + 2\frac{R_2^2}{\zeta^2}dvd\zeta\right) + \frac{r_*^2}{R^2}d\vec{x}^2. \tag{4.2}$$

We consider the scalar field

$$-\frac{1}{\sqrt{-g}}\partial_\mu\left(\sqrt{-g}g^{\mu\nu}\partial_\nu\left(\phi(\zeta)e^{-i\omega v+ikx}\right)\right) = 0. \tag{4.3}$$

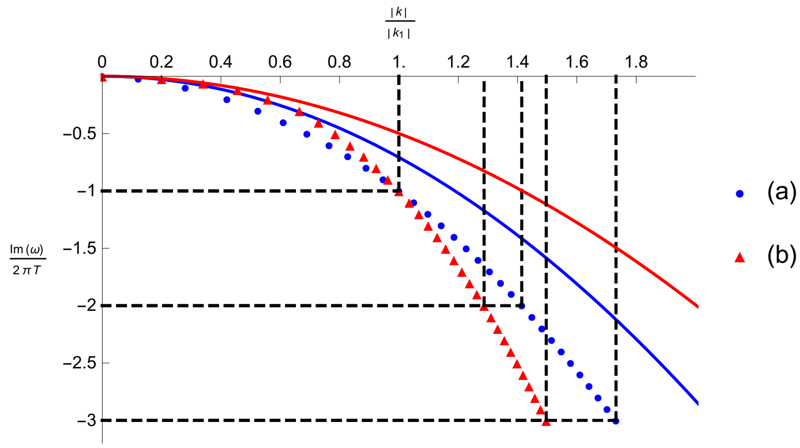

Figure 7. Solid lines show the diffusive hydrodynamic dispersion relation (2.26). The intersections of the dashed lines correspond to the first three order pole-skipping points of axion field $\chi(r)$. Blue dots and red triangles show the curve fitting of pole-skipping points which we choose (a) $z = 2$, $\theta = 3$; (b) $z = 2.5$, $\theta = 3$.

We obtain

$$\phi'' + \frac{2(\zeta - i\omega\zeta_0^2)}{\zeta^2 - \zeta_0^2}\phi' + \frac{4k^2\zeta_0^2}{R_2^2 r_* \zeta^2(\zeta^2 - \zeta_0^2)}\phi = 0. \tag{4.4}$$

Using the method we have mentioned in section 2, we obtain the pole-skipping points located at $\omega = -n2i\pi T$, where n is an integer. The first three order pole-skipping points are

$$\begin{aligned}
&\mathfrak{w}_{\star 1} = -i, && \mathfrak{k}_{\star 1}^2 = 0; \\
&\mathfrak{w}_{\star 2} = -2i, && \mathfrak{k}_{\star 2,1}^2 = 0, && \mathfrak{k}_{\star 2,2}^2 = \frac{\zeta_0^2 R_2^2 r_*}{2}; \\
&\mathfrak{w}_{\star 3} = -3i, && \mathfrak{k}_{\star 3,1}^2 = 0, && \mathfrak{k}_{\star 3,2}^2 = \frac{\zeta_0^2 R_2^2 r_*}{2}, && \mathfrak{k}_{\star 3,3}^2 = \frac{3\zeta_0^2 R_2^2 r_*}{2}; \\
&\mathfrak{w}_{\star 4} = -4i, && \mathfrak{k}_{\star 4,1}^2 = 0, && \mathfrak{k}_{\star 4,2}^2 = \frac{\zeta_0^2 R_2^2 r_*}{2}, && \mathfrak{k}_{\star 4,3}^2 = \frac{3\zeta_0^2 R_2^2 r_*}{2}, && \mathfrak{k}_{\star 4,4}^2 = 3\zeta_0^2 R_2^2 r_*.
\end{aligned} \tag{4.5}$$

In the standard quantization, we set the conformal dimension $\triangle = \frac{1}{2} - \nu$. The retarded Green's function obtained as [35]

$$\mathcal{G}_R = (4\pi T)^{2\nu} \frac{\Gamma(-2\nu)\,\Gamma\left(\frac{1}{2} + \nu - \frac{i\omega}{2\pi T} + iqe_d\right)\Gamma\left(\frac{1}{2} + \nu - iqe_d\right)}{\Gamma(2\nu)\,\Gamma\left(\frac{1}{2} - \nu - \frac{i\omega}{2\pi T} + iqe_d\right)\Gamma\left(\frac{1}{2} - \nu - iqe_d\right)}. \tag{4.6}$$

For convenience to compare with Green's function, we consider the charge of background Q and the external field q to be 0. So the length scale of charge $r_* = 0$ and we do not need to consider the degrees of freedom of momenta ($k_n = 0$). We focus on the locations

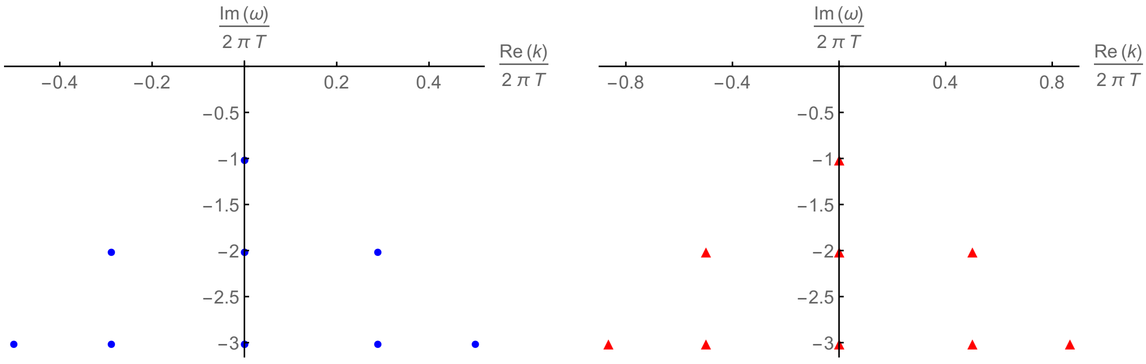

(a) (b)

Figure 8. The first three order pole-skipping points of scalar field $\phi(\zeta)$ in $\mathrm{AdS}_2 \times \mathbb{R}^{d-1}$ geometry (a) $d = 3$, $\zeta_0 = 1$, $R_2 = -\frac{1}{\sqrt{6}}$; (b) $d = 2$, $\zeta_0 = 1$, $R_2 = -\frac{1}{\sqrt{2}}$.

of frequencies of pole-skipping points.

$$
\begin{aligned}
&\text{The zeros of the Green's function are:} \quad \tfrac{1}{2} + \nu - \tfrac{i\omega}{2\pi T} = -\mathrm{i}, \quad \mathrm{i} = 0, 1, 2\ldots, \\
&\text{The poles of the Green's function are:} \quad \tfrac{1}{2} - \nu - \tfrac{i\omega}{2\pi T} = -\mathrm{j}, \quad \mathrm{j} = 0, 1, 2\ldots,
\end{aligned}
$$

where $\nu = \frac{1}{2}$. According to these two equations, the pole-skipping points are located at $\omega = -n2i\pi T$, where n is an integer, which are the same as the results from the near horizon analysis.

The positions of pole-skipping points will not change, whether in the case of standard quantization or alternative quantization [23]. If we consider the alternative quantization, we just take the inverse of $\mathcal{G}_R$ and replace $\triangle \to 1 - \triangle$. After that, we obtain the same special points as the standard quantization.

5 Rindler geometry

The Rindler metric describes the near horizon geometry of a finite-temperature black hole. The ubiquity of the Rindler horizon could be not enough to determine a pole-skipping in the corresponding Green's functions. However, we can use the near horizon analysis to obtain "special points" by making the equation of motion have two incoming solutions. The Rindler metric is given as [36]

$$ds^2 = -K^2\rho^2 dt^2 + d\rho^2 + \frac{1}{4K^2}dx^2 + \frac{1}{4K^2}dy^2, \tag{5.1}$$

where ρ is the proper distance and K is the surface gravity. The Eddington coordinate of the Rindler metric can be written as

$$ds^2 = -K^2\rho^2 dv^2 + 2K\rho dv d\rho + \frac{1}{4K^2}dx^2 + \frac{1}{4K^2}dy^2. \tag{5.2}$$

JHEP06(2021)165

5.1 Sound modes

We consider the sound modes of the metric perturbation

$$h_{vv} = e^{-i\omega v+ikx}h_{vv}(\rho), \qquad h_{vx}= e^{-i\omega v+ikx}h_{vx}(\rho), \tag{5.3}$$

$$h_{xx} = e^{-i\omega v+ikx}h_{xx}(\rho), \qquad h_{yy}= e^{-i\omega v+ikx}h_{yy}(\rho). \tag{5.4}$$

These perturbations have been substituted into the linearized Einstein equation

$$R_{\mu\nu} - \frac{1}{2}Rg_{\mu\nu} = 0. \tag{5.5}$$

We consider the vv component near the horizon

$$k^2h_{vv} + 2k(\omega - iK)h_{vx} + \omega(\omega - iK)(h_{xx} + h_{yy}). \tag{5.6}$$

The lower-half ω-plane of the "special point" is located at

$$\omega_\star = i2\pi T, \qquad k_\star^2 = 0. \tag{5.7}$$

We obtain the Lyapunov exponent $\lambda_L = 2\pi T$ from the "special point", representing the upper-half ω-plane pole-skipping point corresponding to the maximal chaos. This result is the same as the one in Schwarzschild-AdS and Lifshitz geometries.

5.2 Scalar field

For a Klein-Gordon equation

$$-\frac{1}{\sqrt{-g}}\partial_\mu\left(\sqrt{-g}g^{\mu\nu}\partial_\nu\left(\phi(\rho)e^{-i\omega v+ikx}\right)\right) = 0, \tag{5.8}$$

we obtain

$$\phi'' + \frac{K - 2i\omega}{K}\frac{\phi'}{\rho} - 4k^2K^2\phi = 0. \tag{5.9}$$

We calculate the higher order of the "special points" about the scalar field using the method in section 2

$$\omega_{n*} = -in\pi T, \quad k_{n*}^2 = C_n. \quad n = 1, 2, 3\ldots, \quad C_n \text{ are arbitrary constants.} \tag{5.10}$$

So we just determine one parameter ω to ensure two independent incoming wave rather than two parameters ω and k in the Rindler horizon. Equation (5.9) has a singularity at $\rho = 0$. The solution can be written as a Taylor series

$$\phi(\rho) = \rho^\lambda\sum_{n=0}^{\infty}\phi_n\rho^n. \tag{5.11}$$

We can obtain the indicial equation $\lambda(\lambda - \frac{i\omega}{\pi T}) = 0$ and two solutions are

$$\lambda_1 = 0, \quad \lambda_2 = \frac{i\omega}{\pi T}. \tag{5.12}$$

JHEP06(2021)165

If we choose $i\omega = \pi T$ to make the coefficient $(\frac{K-2i\omega}{K})$ vanishing, the two solutions will be

$$\lambda_1 = 0, \quad \lambda_2 = 1. \tag{5.13}$$

In the absence of the boundary condition, it may be not enough to ensure a "pole-skipping" in the corresponding Green's function in the local Rindler structure. However, we can obtain "special points" with two incoming waves from the near horizon in this section. Two incoming solutions correspond to the nonuniqueness of the Green's function. This phenomenon reflects that the pole-skipping points do not depend on the UV property of the Green's function.

6 Discussion and conclusion

In summary, we show that near horizon analysis is a general and simpler method to calculate pole-skipping points. It can not only be applied to AdS spacetime but also Lifshitz and Rindler geometry. The pole-skipping points are related to the hydrodynamic dispersion relations in the small ω and k regime. We calculate the lower-half ω-plane pole-skipping points of tensor and Maxwell fields in the anisotropic system near the Lifshitz critical points. The frequencies of these special points are located at $\mathfrak{w}_n = -in$ with n integers. To verify our results, we compare them with outcomes of the AdS_4 black brane solution in refs. [13, 14] when setting $z = 1$, $\theta = 0$ and $\phi = 1$. They are the same at the first order pole-skipping point ($\mathfrak{w}_n = -i$). The momenta k_n of higher-order pole-skipping points are in the complex k-plane. We plot the dispersion relations in terms of dimensionless variables $\frac{\omega}{2\pi T}$ and $\frac{|k|}{2\pi T}$. We find that the hydrodynamic dispersion relations pass through pole-skipping points $(\mathfrak{w}_n, |\mathfrak{k}_n|)$ at the minimal momentum and frequency. For the hydrodynamic analysis, we just consider the linearized perturbations along with the directions of translation-invariant symmetry, which are the cases of non dissipated momenta ($a = 0$) and conserved U(1) currents. In ref. [25], the authors calculate the pole skipping points in anisotropic plasma ($a \neq 0$), and they compute the dispersion relation for momentum diffusion and show that it passes through the first three successive pole skipping points.

The axion field was shown with the same phenomenon in the Lifshitz black hole background with a linear axion field and a hyperscaling violating factor. The lower half-plane pole-skipping points at negative integer (imaginary) Matsubara frequencies. When $\theta = 0$, $z = 1$, $Q = 0$ and $\beta = 0$, the metric (3.2) recovers the AdS_4 black brane solution. The location of the first order pole-skipping point is the same as that of refs. [13, 14]. We also compare the lower half-plane pole-skipping points with hydrodynamic poles showing that the hydrodynamic dispersion relation passes through pole-skipping points when $\mathfrak{w}, \mathfrak{k} \to 0$.

We calculate the pole-skipping points of a scalar field in the background of $\mathrm{AdS}_2 \times \mathbb{R}^{d-1}$. When we choose the different quantization, the locations of pole-skipping points are not changed, although this phenomenon has been already found in ref. [23]. It is a general conclusion in all background.

We cannot obtain poles-kipping points by solving Green's function directly because of the lack of boundary conditions in Rindler geometry. Nevertheless, near the horizon, we can obtain the "special points" by solving the bulk equations of motion. Two incoming waves at these "special points" consist of poles-kipping points obtained by solving Green's function.

We wish to verify that it is a general conclusion that the pole-skipping points are related to the hydrodynamic dispersion relation, especially in the anisotropic geometry along the direction in which momentum is dissipated. We are also interested in why the "pole-skipping" points can be obtained without boundary conditions in Rindler geometry or other systems. It may have important research significance in holography.

Acknowledgments

We would like to thank Keun-Young Kim, Matteo Baggioli, Yan Liu, Yu-Qi Lei, and Qing-Bing Wang for helpful discussions. This work is partly supported by NSFC (No.11875184).

A Details of near-horizon expansions

In this appendix, we show the details of the near-horizon expansions of the equations of motion.

A.1 Anisotropic system near Lifshitz points

We can calculate a Taylor series solution to the tensor mode h^x_y, Maxwell vector mode A_y equations of motion when the matrix equation (2.21) is satisfied. For the convenience of numerical calculation, we set the horizon radius $r_+ = 1$ and $L = 1$. The first few elements of this matrix are shown below.

A.1.1 Tensor mode (a=0)

For the perturbation along x-direction of tensor mode h^x_y in equation (2.11) with $a = 0$, the first few elements of this matrix are

$$\begin{aligned}
M_{11} &= -\frac{1}{2r_+}\Big\{k^2 Lr_+ + i\omega(\theta-2)\Big\},\\
M_{21} &= -\frac{1}{2r_+^2}\Big\{2k^2 Lr_+ + i\omega(\theta-2)\Big\},\\
M_{22} &= -\frac{1}{2r_+}\Big\{k^2 Lr_+ - 4\pi T\theta + i\omega(\theta+2)\Big\} + \frac{f''(r_+)}{2L},\\
M_{31} &= -\frac{k^2 L}{r_+^2},\\
M_{32} &= \frac{1}{2Lr_+^2}\Big\{-2L(2k^2 Lr_+ - 4\pi T(\theta-1) + i\omega\theta) + r_+(\theta+2)f''(r_+) + r_+^2 f^{(3)}(r_+)\Big\},\\
M_{33} &= -\frac{1}{2r_+}\Big\{k^2 Lr_+ - 8\pi T(\theta-2) + i\omega(6+\theta)\Big\} + \frac{3f''(r_+)}{2L}.
\end{aligned}$$

A.1.2 Tensor mode ($a \neq 0$)

For the perturbation along x-direction of tensor mode h_y^x in equation (2.28) with $a \neq 0$, the first few elements of this matrix are

$$\begin{aligned}
M_{11} &= -\frac{1}{2r_+}\Big\{k^2 L r_+^{\phi} + a^2 L r_+^{2\kappa\lambda+\phi} + i\omega(1+\theta-3\phi)\Big\},\\
M_{21} &= -\frac{1}{2r_+^2}\Big\{2k^2 L r_+^{\phi}\phi + 2a^2 L r_+^{2\kappa\lambda+\phi}(\kappa\lambda+\phi) + i\omega\phi(1+\theta-3\phi)\Big\},\\
M_{22} &= -\frac{1}{2r_+ L}\Big\{L(k^2 L r_+^{\phi} + a^2 L r_+^{2\kappa\lambda+\phi} - 4\pi T(4+\theta-4\phi) + i\omega(3+\theta-\phi)) - r_+^{2-\phi} f''(r_+)\Big\},\\
M_{31} &= -\frac{1}{2r_+^3}\Big\{2a^2 L r_+^{2\kappa\lambda+\phi}(2\kappa^2\lambda^2 + \phi(2\phi-1) + \kappa\lambda(4\phi-1)) + \phi(2k^2 L r_+^{\phi}(2\phi-1)\\
&\quad + i\omega(1+\theta-3\phi)(\phi-1))\Big\},\\
M_{32} &= \frac{r_+^{2-\phi}}{2L}\Big\{-2L r_+^{\phi}(-4\pi T(3+\theta-4\phi) + 2k^2 L r_+^{\phi}\phi + 2a^2 L r_+^{2\kappa\lambda+\phi}(\kappa\lambda+\phi) + i\omega\phi(2+\theta-2\phi))\\
&\quad + r_+^2(6+\theta-4\phi) f''(r_+) + r_+^3 f^{(3)}(r_+)\Big\},\\
M_{33} &= -\frac{1}{2r_+}\Big\{k^2 L r_+^{\phi} + a^2 L r_+^{2\kappa\lambda+\phi} - 8\pi T(6+\theta-4\phi) + i\omega(5+\theta+\phi)\Big\} + \frac{3r_+^{1-\phi} f''(r_+)}{2L}.
\end{aligned}$$

A.1.3 Maxwell vector mode

For the Maxwell vector A_y in the equation of motion (2.41), the first few elements of this matrix are

$$\begin{aligned}
M_{11} &= \frac{1}{2}\Big\{-k^2 - i\omega(1+2\zeta\kappa-\phi)\Big\},\\
M_{21} &= \frac{1}{4}\Big\{-2k^2\phi - i\omega z(1+2\zeta\kappa-\phi)\Big\},\\
M_{22} &= \frac{1}{4}\Big\{-k^2 - 4\pi T(z-2\zeta\kappa-\phi-4) - i\omega(3+2z+\zeta\kappa-\phi) + f''(1)\Big\},\\
M_{31} &= \frac{1}{12}\Big\{-2k^2\phi(2\phi-1) - z(z-1)i\omega(1+2\zeta\kappa-\phi)\Big\},\\
M_{32} &= \frac{1}{12}\Big\{-4k^2\phi - 8\pi T(z+\phi-2\zeta\kappa-3) - 2zi\omega(z+2\zeta\kappa+2-\phi) - (z+\phi-2\zeta\kappa-6)f''(1)\\
&\quad + f^{(3)}(1)\Big\},\\
M_{33} &= \frac{1}{6}\{-k^2 - 8\pi T(z-\zeta\kappa+\phi-6) - i\omega(4z+2\zeta\kappa-\phi+5) + 3f''(1)\}.
\end{aligned}$$

A.2 Lifshitz black hole with linear axion fields and hyperscaling violating factor

We can calculate a Taylor series solution to the equation of axion field $\chi(r)$ (3.8) when the matrix equation (3.18) is satisfied. For convenience, we set the horizon radius $r_H = 1$.

The first few elements of this matrix are

$$
\begin{aligned}
M_{11} &= \frac{1}{2}\Big\{-k^2+i\omega(\delta+\theta-2)\Big\},\\
M_{21} &= \frac{1}{4}\Big\{4k^2-i\omega(z+2)(\delta+\theta-2)\Big\},\\
M_{22} &= \frac{1}{4}\Big\{-k^2+i\omega(\delta+\theta-2)-4\pi T(\delta+\theta-z-3)+2i\omega(z+1)+f''(1)\Big\},\\
M_{31} &= \frac{1}{12}\Big\{-20k^2+i\omega(z+2)(z+3)(\delta+\theta-2)\Big\},\\
M_{32} &= \frac{1}{12}\Big\{8k^2-2i\omega(z+2)(\delta+\theta-2)-2i\omega(z+1)(z+2)+(\delta+\theta-z-3)(8\pi T-f''(1))\\
&\qquad +f^{(3)}(1)\Big\},\\
M_{33} &= \frac{1}{6}\Big\{-k^2+i\omega(\delta+\theta-2)+f''(1)-8\pi T(\delta+\theta-z-3)+4i\omega(z+1)+2f''(1)\Big\}.
\end{aligned}
$$

A.3 $\mathrm{AdS}_2 \times \mathbb{R}^{d-1}$ geometry

For the scalar field ϕ in the equation of motion (4.4), the first few elements of this matrix are

$$
\begin{aligned}
M_{11} &= \frac{4k^2\pi^2T^2}{R_2^2 r_*}, \qquad\qquad M_{21} = 0,\\
M_{22} &= \frac{2\pi T(2k^2\pi T + R_2^2 r_*(3\pi T - i\omega))}{R_2^2 r_*},\\
M_{31} &= 0, \qquad\qquad M_{32} = 4\pi^2T^2(6\pi T - i\omega),\\
M_{33} &= \frac{4\pi T(2k^2\pi T + R_2^2 r_*(11\pi T - 2i\omega))}{3R_2^2 r_*},\\
M_{41} &= 0, \qquad\qquad M_{42} = 4\pi^4T^4,\\
M_{43} &= 2\pi^2T^2(10\pi T - i\omega),\\
M_{44} &= \frac{2k^2\pi^2T^2 + 24\pi^2T^2R_2^2 r_* - 3i\omega\pi T R_2^2 r_*}{R_2^2 r_*}.
\end{aligned}
$$

References

[1] J.M. Maldacena, *The Large N limit of superconformal field theories and supergravity*, *Int. J. Theor. Phys.* **38** (1999) 1113 [hep-th/9711200] [INSPIRE].

[2] E. Witten, *Anti-de Sitter space and holography*, *Adv. Theor. Math. Phys.* **2** (1998) 253 [hep-th/9802150] [INSPIRE].

[3] E. Witten, *Anti-de Sitter space, thermal phase transition, and confinement in gauge theories*, *Adv. Theor. Math. Phys.* **2** (1998) 505 [hep-th/9803131] [INSPIRE].

[4] S.S. Gubser, I.R. Klebanov and A.M. Polyakov, *Gauge theory correlators from noncritical string theory*, *Phys. Lett. B* **428** (1998) 105 [hep-th/9802109] [INSPIRE].

[5] J. Casalderrey-Solana, H. Liu, D. Mateos, K. Rajagopal and U.A. Wiedemann, *Gauge/String Duality, Hot QCD and Heavy Ion Collisions*, Cambridge University Press (2014) [DOI] [arXiv:1101.0618] [INSPIRE].

[6] M. Natsuume, *AdS/CFT Duality User Guide*, vol. 903 (2015), [DOI] [arXiv:1409.3575] [INSPIRE].

[7] M. Ammon and J. Erdmenger, *Gauge/gravity duality: Foundations and applications*, Cambridge University Press (2015) [DOI].

[8] J. Zaanen, Y.W. Sun, Y. Liu and K. Schalm, *Holographic Duality in Condensed Matter Physics*, Cambridge University Press (2015) [DOI].

[9] S.A. Hartnoll, A. Lucas and S. Sachdev, *Holographic quantum matter*, The MIT Press (2018) [arXiv:1612.07324].

[10] S.H. Shenker and D. Stanford, *Black holes and the butterfly effect*, *JHEP* **03** (2014) 067 [arXiv:1306.0622] [INSPIRE].

[11] D.A. Roberts, D. Stanford and L. Susskind, *Localized shocks*, *JHEP* **03** (2015) 051 [arXiv:1409.8180] [INSPIRE].

[12] S.H. Shenker and D. Stanford, *Stringy effects in scrambling*, *JHEP* **05** (2015) 132 [arXiv:1412.6087] [INSPIRE].

[13] M. Natsuume and T. Okamura, *Holographic chaos, pole-skipping, and regularity*, *PTEP* **2020** (2020) 013B07 [arXiv:1905.12014] [INSPIRE].

[14] M. Natsuume and T. Okamura, *Nonuniqueness of Green's functions at special points*, *JHEP* **12** (2019) 139 [arXiv:1905.12015] [INSPIRE].

[15] S. Grozdanov, K. Schalm and V. Scopelliti, *Black hole scrambling from hydrodynamics*, *Phys. Rev. Lett.* **120** (2018) 231601 [arXiv:1710.00921] [INSPIRE].

[16] M. Blake, R.A. Davison, S. Grozdanov and H. Liu, *Many-body chaos and energy dynamics in holography*, *JHEP* **10** (2018) 035 [arXiv:1809.01169] [INSPIRE].

[17] S. Grozdanov, *On the connection between hydrodynamics and quantum chaos in holographic theories with stringy corrections*, *JHEP* **01** (2019) 048 [arXiv:1811.09641] [INSPIRE].

[18] M. Blake, R.A. Davison and D. Vegh, *Horizon constraints on holographic Green's functions*, *JHEP* **01** (2020) 077 [arXiv:1904.12883] [INSPIRE].

[19] M. Natsuume and T. Okamura, *Pole-skipping with finite-coupling corrections*, *Phys. Rev. D* **100** (2019) 126012 [arXiv:1909.09168] [INSPIRE].

[20] S. Das, B. Ezhuthachan and A. Kundu, *Real time dynamics from low point correlators in 2d BCFT*, *JHEP* **12** (2019) 141.

[21] N. Abbasi and J. Tabatabaei, *Quantum chaos, pole-skipping and hydrodynamics in a holographic system with chiral anomaly*, *JHEP* **03** (2020) 050 [arXiv:1910.13696] [INSPIRE].

[22] N. Abbasi and S. Tahery, *Complexified quasinormal modes and the pole-skipping in a holographic system at finite chemical potential*, *JHEP* **10** (2020) 076 [arXiv:2007.10024] [INSPIRE].

[23] Y. Ahn, V. Jahnke, H.-S. Jeong, K.-Y. Kim, K.-S. Lee and M. Nishida, *Pole-skipping of scalar and vector fields in hyperbolic space: conformal blocks and holography*, *JHEP* **09** (2020) 111 [arXiv:2006.00974] [INSPIRE].

[24] C. Choi, M. Mezei and G. Sárosi, *Pole skipping away from maximal chaos*, arXiv:2010.08558 [INSPIRE].

[25] K. Sil, *Pole skipping and chaos in anisotropic plasma: a holographic study*, *JHEP* **03** (2021) 232 [arXiv:2012.07710] [INSPIRE].

[26] Y. Ahn, V. Jahnke, H.-S. Jeong, K.-S. Lee, M. Nishida and K.-Y. Kim, *Classifying pole-skipping points*, *JHEP* **03** (2021) 175 [arXiv:2010.16166] [INSPIRE].

[27] N. Iqbal and H. Liu, *Universality of the hydrodynamic limit in AdS/CFT and the membrane paradigm*, *Phys. Rev. D.* **79** (2009) 025023 [arXiv:0809.3808].

[28] S. Grozdanov, P.K. Kovtun, A.O. Starinets and P. Tadić, *The complex life of hydrodynamic modes*, *JHEP* **11** (2019) 097 [arXiv:1904.12862] [INSPIRE].

[29] G.A. Inkof, J.M.C. Küppers, J.M. Link, B. Goutéraux and J. Schmalian, *Quantum critical scaling and holographic bound for transport coefficients near Lifshitz points*, *JHEP* **11** (2020) 088 [arXiv:1907.05744] [INSPIRE].

[30] X.-H. Ge, Y. Tian, S.-Y. Wu, S.-F. Wu and S.-F. Wu, *Linear and quadratic in temperature resistivity from holography*, *JHEP* **11** (2016) 128 [arXiv:1606.07905] [INSPIRE].

[31] X.-H. Ge, Y. Tian, S.-Y. Wu and S.-F. Wu, *Hyperscaling violating black hole solutions and Magneto-thermoelectric DC conductivities in holography*, *Phys. Rev. D* **96** (2017) 046015 [*Erratum ibid.* **97** (2018) 089901] [arXiv:1606.05959] [INSPIRE].

[32] X.-H. Ge, S.-J. Sin and S.-F. Wu, *Universality of DC Electrical Conductivity from Holography*, *Phys. Lett. B* **767** (2017) 63 [arXiv:1512.01917] [INSPIRE].

[33] Z.-N. Chen, X.-H. Ge, S.-Y. Wu, G.-H. Yang and H.-S. Zhang, *Magnetothermoelectric DC conductivities from holography models with hyperscaling factor in Lifshitz spacetime*, *Nucl. Phys. B* **924** (2017) 387 [arXiv:1709.08428] [INSPIRE].

[34] B. Goutéraux, *Charge transport in holography with momentum dissipation*, *JHEP* **04** (2014) 181 [arXiv:1401.5436] [INSPIRE].

[35] T. Faulkner, H. Liu, J. McGreevy and D. Vegh, *Emergent quantum criticality, Fermi surfaces, and AdS$_2$*, *Phys. Rev. D* **83** (2011) 125002 [arXiv:0907.2694] [INSPIRE].

[36] Robert M. Wald, *General Relativity*, University Of Chicago Press (1984) [DOI].

JHEP06(2021)165